

Communication

A Study on Alpha-Case Depth in Ti-6Al-2Sn-4Zr-2Mo

KEVIN S. McREYNOLDS
and SESHACHARYULU TAMIRISAKANDALA

Isothermal oxidation experiments in air were performed on Ti-6Al-2Sn-4Zr-2Mo (Ti-6242) with a bimodal microstructure in the temperature range 811 K to 922 K (538 °C to 649 °C) for up to 500 hours, and α -case depths were quantified using metallography. Alpha-case depth followed a parabolic variation with time. Alpha-case depths in excess of 10 μm formed above 811 K (538 °C) and 100-hour exposures. An activation energy of 244 kJ/mol was estimated for diffusion of oxygen in the α phase of Ti-6242.

DOI: 10.1007/s11661-011-0710-3

© The Minerals, Metals & Materials Society and ASM International 2011

The high chemical affinity of titanium to oxygen (indicated by Ti-O bond energy of 2.12 eV, comparable to the Ti-Ti bond energy of 2.56 eV^[1]) and the high interstitial solid solubility of oxygen in α -titanium (about 14.5 wt pct or 34 at. pct in pure titanium^[2]) cause significant oxygen ingress during air exposure at high temperatures, resulting in the simultaneous formation of an oxide (TiO₂) scale on the surface and an oxygen-rich α layer underneath the scale. Formation of an oxygen-rich α layer is a result of the oxygen gradient, oxygen migration through the n -type anion-defective TiO₂ scale, and the relative ease of interstitial diffusion. This layer is commonly referred to as α case, since it is a continuous, hard, and brittle zone of oxygen-stabilized α phase. Alpha-case forms during casting,^[3] processing,^[4] and elevated temperature exposure in service. Alpha-case formed during casting or processing is completely removed *via* machining or chemical milling.^[5] Alpha-case formed during service often limits the maximum service temperature of titanium alloys, since a significant amount of less ductile α case results in the formation of surface cracks under tensile loading. Incorporation of oxygen leads to anisotropic lattice distortions, thus hindering dislocation mobility and changing the deformation behavior from a wavy to a planar slip mode.^[6] The low local ductility and the large slip offsets at the

surface can cause low overall ductility or early crack nucleation under cyclic loading conditions.

The service conditions that affect the oxidation kinetics are environment, temperature, stress, and exposure time. For long-term elevated-temperature applications such as blades, disks, and impellers in gas turbine aero-engines, α -case depth is critically important in addition to creep resistance and strength.^[7] For short-term elevated-temperature applications such as thermal protection systems and hot structures that include thin-wall components, rapid degradation across the entire cross section could occur due to α -case formation.^[8] The high-temperature application of conventional titanium alloys is therefore limited to a temperature regime below which diffusion rates through the oxide scale are slow enough to prevent excess oxygen content being dissolved in the bulk material, resulting in no significant α -case depth.

While the α -case formation and its deleterious effects on component life are well known,^[9] quantitative studies on α case are scant. Shamblen and Redden^[10] determined the air contamination rates using microhardness traverses and approximated diffusion of oxygen in the α phase of high-temperature titanium alloy Ti-6Al-2Sn-4Zr-2Mo (Ti-6242, all compositions are given in weight percent unless noted otherwise) bar stock based on a relationship between oxygen concentration and microhardness. Shenoy *et al.*^[8] studied the oxidation kinetics in Ti-6242 sheet and foil using thermogravimetric analysis and estimated the substrate contamination from empirical relations using weight gain and microhardness measurements. Similar studies were performed on other high-temperature Ti alloys Ti-5.8Al-4Sn-3.5Zr-0.5Mo-0.7Nb-0.35Si-0.06C (IMI 834)^[11] and Ti-6Al-2.7Sn-4Zr-0.4Mo-0.45Si (Ti-1100).^[12] Indirect measurements of α case can be made for penetration depths that are sufficiently large for microindentations, and weight gains due to oxygen enrichment are significantly high. Structural titanium components are never operated at service conditions that lead to large α -case depths due to the risk of catastrophic failures. Measurement of small α -case depths that form at service conditions are of interest from a design viewpoint. This enables introduction of α -case depth as a design parameter into damage nucleation and growth models for predicting component life under service conditions and developing fail-safe designs. Since the oxidation attack is limited to the outer region of components, whereas mechanical properties at elevated temperatures are determined by the bulk cross section, a promising approach would be to optimize both mechanical properties and oxidation resistance. A quantitative model of α -case depth would be helpful for this purpose. The objective of this study is therefore to quantify α -case depth in service temperature and time ranges of interest. Such data would be useful to those working in the field, especially in making engineering assessments. Experiments were conducted on the most commonly used high-temperature titanium alloy Ti-6242. Isothermal oxidation experiments were performed in the temperature range 811 K to 922 K (538 °C to 649 °C) up to 500 hours, and α -case depths were quantified using a metallographic technique.

KEVIN S. McREYNOLDS, Student, is with UES, Inc., Dayton, OH 45432. SESHACHARYULU TAMIRISAKANDALA, Senior Scientist, is with FMW Composite Systems, Inc., Bridgeport, WV 26330. Contact e-mail: seshacharyulu.tamirisakandala.ctr@wpafb.af.mil
Manuscript submitted November 8, 2010.

Article published online April 26, 2011

The material used for the oxidation experiments was a standard Ti-6242 (complete chemical analysis given in Table I) annealed bar of 25.4-mm diameter supplied by ATI Allvac.^[13] Samples of $10 \times 5 \times 10 \text{ mm}^3$ with the 10-mm side along the longitudinal direction of the bar were cut using electrical discharge machining (EDM), and all faces were low stress ground to remove the recast layer formed after EDM. Static isothermal oxidation experiments at atmospheric pressure were performed in a laboratory air furnace at 811 K, 866 K, and 922 K (538 °C, 593 °C, and 649 °C). Samples were taken out after 5, 10, 50, 100, and 500 hours of exposure at each temperature. The weight change of each sample after thermal exposure was measured using a microbalance with reproducibility of $\pm 0.0001 \text{ g}$. Samples were then sectioned at midheight, parallel to the furnace contact face. Cut faces of $5 \times 10 \text{ mm}^2$ were metallographically polished and etched by immersing in oxalic tint etchant consisting of 2 mL HF and 98 mL saturated aqueous $\text{C}_2\text{H}_2\text{O}_4$. The tint etch stained the microstructure and revealed interstitial-enriched α case as a relatively bright layer. The etchant was freshly made in each case, and etch conditions were kept constant for all samples. Alpha-case region was imaged using optical microscopy. A statistically significant number of measurements of α -case depth in each sample were made along the entire perimeter at approximately 500- μm spacing. The plane of examination included two longitudinal and two transverse sides of the Ti-6242 bar, and the average α -case depth from 60 individual measurements on each sample is reported. Scanning electron microscopy was also used to examine microstructures of selected samples. Vickers microhardness measurements were made for verification purposes using a diamond square pyramid indenter and 100 gf load (diagonal lengths of indents in the range 19 to 25 μm) on 500-hour exposed

samples. Elemental concentration profiles in α -case regions were obtained from electron probe microanalysis (EPMA) using 15 keV and 40 nA probe.

The starting microstructure of Ti-6242 used in this study, shown in Figure 1, consisted of a bimodal (mix of equiaxed and lamellar $\alpha + \beta$) morphology with primary α volume fraction of 0.47, average primary α grain size of 6 μm , lamellar α volume fraction of 0.27, and β -phase volume fraction of 0.26. Bimodal microstructure is typically used for fracture-critical applications to obtain an optimum balance of creep resistance and fatigue resistance.^[14] Microstructural features were similar in both the longitudinal and transverse orientations of the bar, except that primary α grains were slightly elongated along the longitudinal orientation. The weight change normalized by the surface area of each specimen after thermal exposure at different temperatures and times is plotted in Figure 2. All samples gained weight in the temperature and time ranges considered. The weight gain increased with increasing time and temperature. The variation of weight gain with time approximately followed a parabolic relationship.

An example of α -case microstructure for the sample exposed at 922 K (649 °C) for 50 hours, etched with oxalic tint etchant, is shown in Figure 3. Alpha-case, consisting of a group of oxygen-enriched α grains, appears as a bright band near the edge of the sample in this micrograph. A montage created by an array of optical micrographs on this sample is included in this figure, which reveals a continuous α case along the entire periphery of the sample. Alpha-case depth was fairly uniform in both the longitudinal and transverse directions. A secondary electron image obtained near the edge of the sample is also shown in Figure 3, which reveals an oxide scale approximately 1- μm thick above the α case. Oxide scale thickness was in the range 1 to

Table I. Chemical Composition of Ti-6Al-2Sn-4Zr-2Mo Material Used for Oxidation Study

Al	Sn	Zr	Mo	Si	Fe	Ni	C	O	N	H	Ti
6.10	1.76	4.16	2.08	0.066	0.048	0.037	0.019	0.132	0.027	0.0051	bal

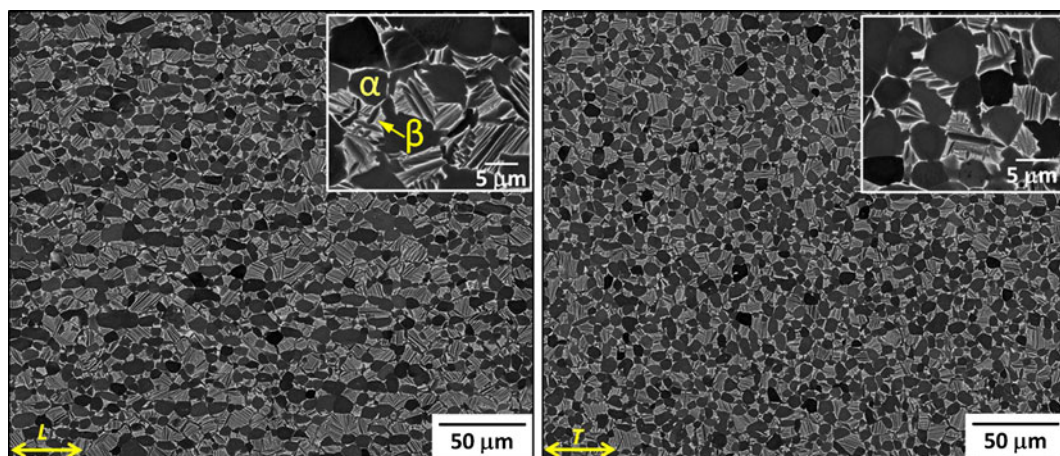


Fig. 1—Starting microstructure of Ti-6242 bar (in longitudinal *L* and transverse *T* orientations) used for isothermal oxidation experiments.

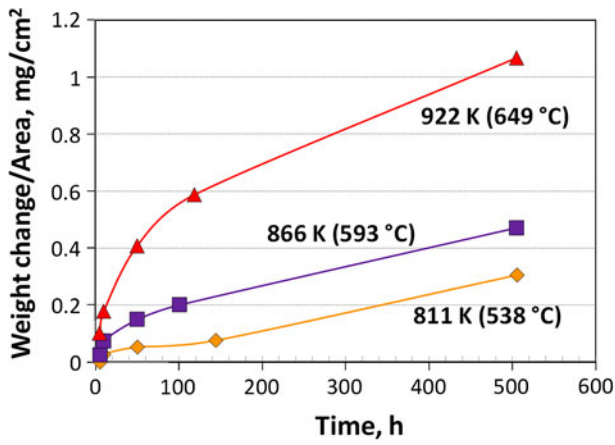


Fig. 2—Weight change of Ti-6242 samples as a function of time at different temperatures of isothermal exposure.

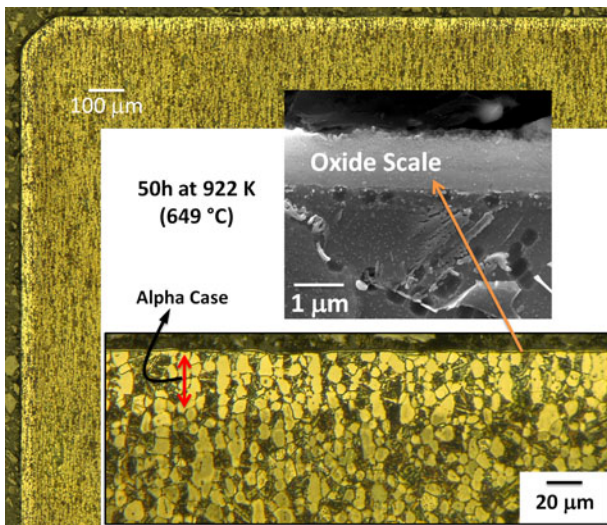


Fig. 3—Micrographs of Ti-6242 sample exposed at 922 K (649 °C) for 50 h, revealing subsurface α case (optical micrographs obtained on oxalic tint-etched surface) around the perimeter and oxide scale (secondary electron image) on the surface.

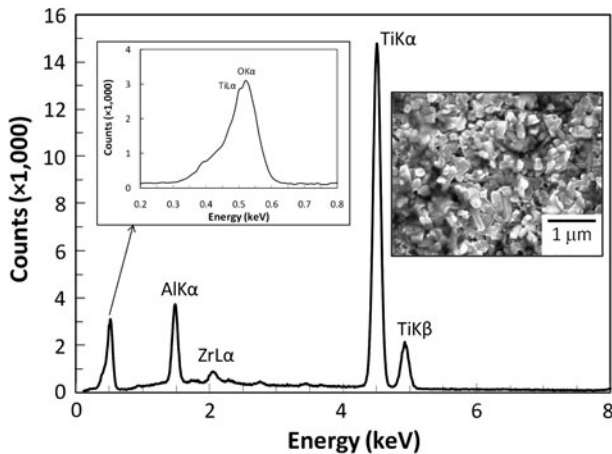


Fig. 4—Energy-dispersive X-ray spectroscopy spectrum obtained on oxide scale that formed on sample exposed at 922 K (649 °C) for 500 h.

3.5 μm for the temperature and time ranges considered in this study. Typical energy-dispersive X-ray spectroscopy spectrum obtained on the oxide scale is presented in Figure 4, which shows the presence of Ti, O, Al, and Zr. Alpha case could not be distinguished in scanning electron micrographs, either in the secondary or the backscattered electron imaging mode, as sufficient contrast is not created by the higher oxygen concentration in α case compared to the base metal. A gradient in oxygen concentration within α -case depth occurs, dropping from the solubility limit to the bulk concentration in the base metal. Elemental concentration profiles obtained from EPMA line scans of 1- μm step size along the depth of the sample exposed at 922 K (649 °C) for 500 hours are presented in Figure 5(a). Enlarged oxygen concentration profile is shown in Figure 5(b). Backscattered electron image of the EPMA line scan region with optical measurement of α -case depth ($82 \pm 5 \mu\text{m}$) marked is shown Figure 5(c). Oxygen concentration was about 4 wt pct adjacent to the oxide scale, dropped to about 0.10 wt pct (close to the bulk concentration) at a depth of 55 μm , and remained constant thereafter. Shenoy *et al.*^[8] determined that the maximum interstitial solid solubility of oxygen in the α phase of Ti-6242 is about 2.37 wt pct (7 at. pct) compared to 14.5 wt pct (34 at. pct) in pure α -Ti, which is in agreement with the present analysis. The EPMA analysis verified that oxalic tint etch contrast captures the entire α -case region. This assumption was also verified to be accurate using nanoindentation measurements as a function of depth in a similar material.^[15] Concentration profile of nitrogen, another potential α -case forming element, from EPMA is also shown in Figure 5(a). Nitrogen concentration was constant along the depth, indicating the absence of nitrogen ingress in the α -case region. Microstructural analysis confirmed the absence of any nitrides in α -case.

Alpha-case microstructures of samples at different temperature-time combinations are compared in Figure 6. Average α -case depth along with standard deviation is plotted against exposure time for each temperature in Figure 7. At 811 K (538 °C) exposure, α -case depth is small, about 15 μm after 500 hours. Above 811 K (538 °C), significantly thicker α -case formed. Ten hours exposure at 922 K (649 °C) resulted in an α -case depth that is approximately the same for a 500-hour exposure at 811 K (538 °C). Alpha-case depth variation with time at all three temperatures followed parabolic relationships.

Microhardness measurements taken on 500-hour exposure samples are shown in Figure 8. Microhardness indents were made as close to the edge as possible without cracking the sample. For the sample oxidized at 811 K (538 °C), the indent size was comparable to the depth of α -case. Vickers microhardness of α -case is about 50 points higher than that of the base metal. Microhardness of α -case in the sample exposed at 922 K (649 °C) was about 100 points higher than that for samples exposed at 811 K or 866 K (538 °C or 593 °C) for the same time, which could be due to the difference in oxygen concentration in the α -case at the location of microindentation. Though care is taken to measure

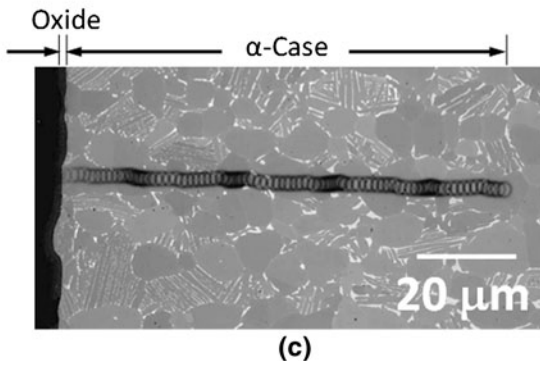
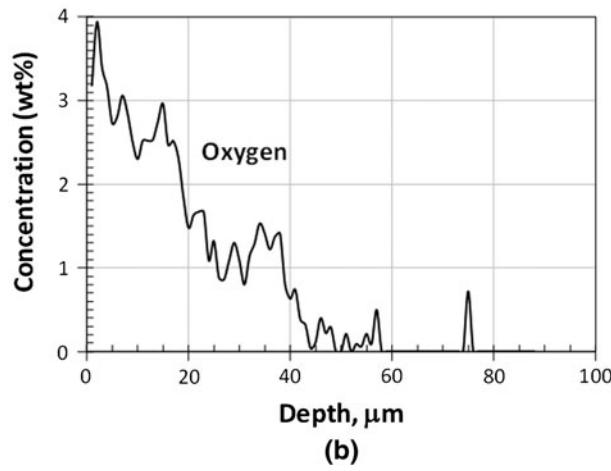
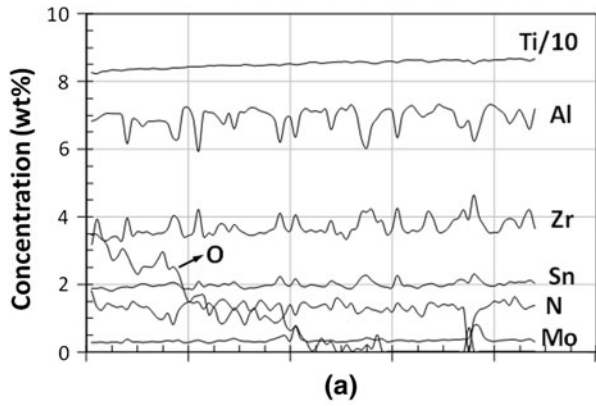


Fig. 5—(a) EPMA elemental concentration profiles along the depth of 922 K (649 °C)/500 h oxidized sample from a line scan of 1- μ m step size. (b) Enlarged oxygen concentration profile. (c) Backscattered electron image of the EPMA scan region with optical measurement of α -case marked.

microhardness at the same location in each sample, absolute comparison of values may not be accurate. For the lowest exposure temperature at which the indent size is comparable to α -case depth, hardness will be an average across the depth, whereas values at the higher temperatures will depend on the oxygen content at the indent location within the α -case. Microhardness of the base metal shows softening behavior with an increase in exposure temperature, which is likely due to the change in microstructure caused by coarsening and dissolution of Ti_3Al precipitates.^[7]

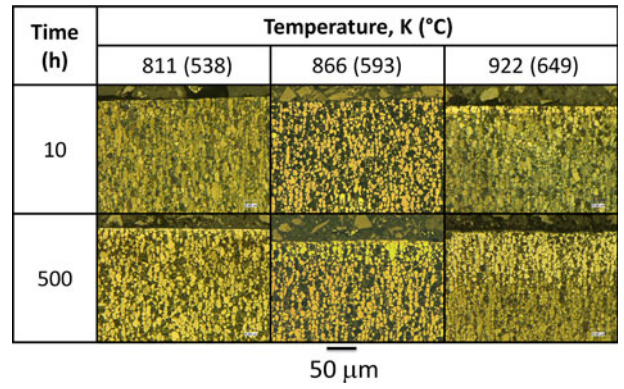


Fig. 6—Micrographs (optical images obtained on oxalic tint-etched surface) of Ti-6242 samples exposed at different temperatures and times comparing α -case depth.

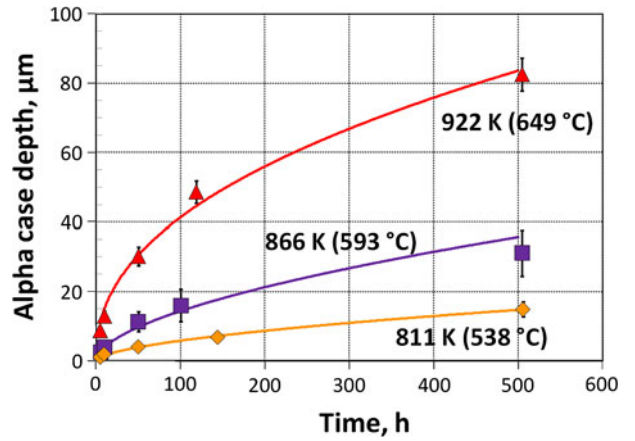


Fig. 7—Variation of Ti-6242 α -case depth as a function of time at different temperatures.

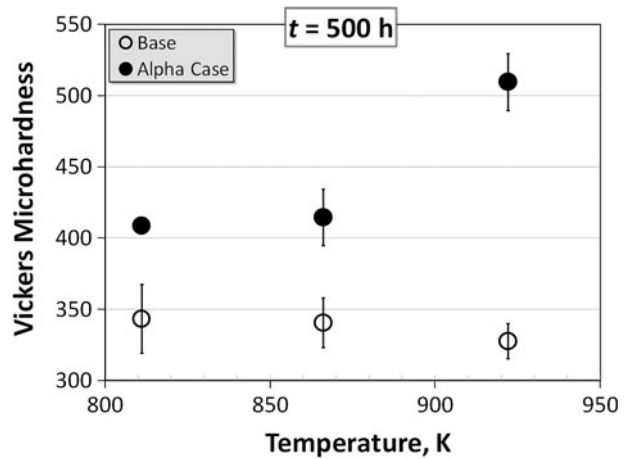


Fig. 8—Vickers microhardness measurements in the base and α -case regions of Ti-6242 oxidized at different temperatures for 500 h.

Considering the shallow depths of α -case in relation to specimen dimensions, it is reasonable to assume that the specimens are of semi-infinite thickness and that an

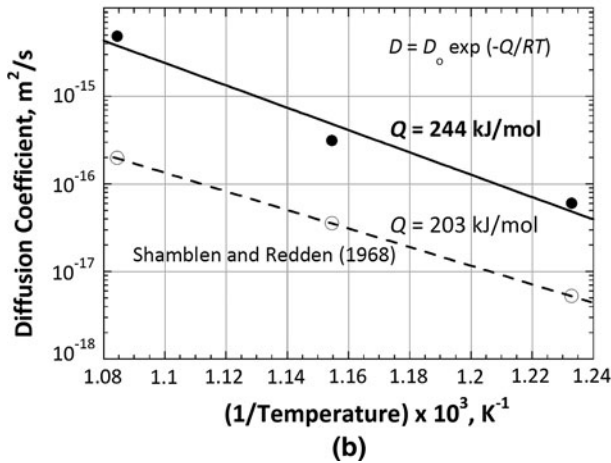
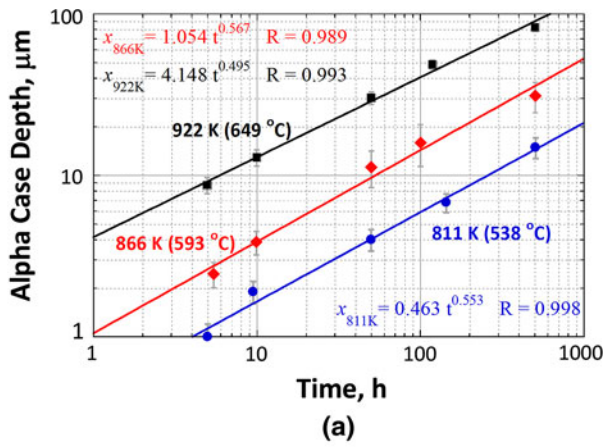


Fig. 9—(a) Log-log plot of α -case depth vs time used for the determination of diffusion coefficients. (b) Semilog plot of diffusion coefficient vs inverse of absolute temperature used for the estimation of activation energy.

approximate solution for Fick's second law of diffusion $x = \sqrt{Dt}$ applies, where x is α -case depth, D is the diffusion coefficient, and t is exposure time. Log-log plots of x vs t , shown in Figure 9(a), reveal linear trends with excellent correlation coefficients of 0.99. The exponents from these linear fits were close to 0.5. The D values calculated from the best-fit lines are plotted against the reciprocal of absolute temperatures (T) in Figure 9(b). The D vs $(1/T)$ variation follows an Arrhenius-type relationship, $D = D_0 \exp(-Q/RT)$, where D_0 is the pre-exponent factor, Q is the activation energy for diffusion of oxygen in the α phase, and R is the gas constant. From the best-fit line, Q was calculated to be 244 kJ/mol. The D values approximated by Shamblen and Redden^[10] are also plotted in Figure 9(b), which are about an order magnitude lower than the values obtained in the current study, and the estimated Q was 203 kJ/mol. Differences in D and Q could be attributed to the influence of the starting microstructure on the diffusion of oxygen in Ti-6242, errors associated with correlation between microhardness and α -case

depth, and sensitivity of the oxalic acid tint etch to the oxygen content in reproducibly identifying the full depth of α case.

In summary, α -case depth as a function of time in Ti-6Al-2Sn-4Zr-2Mo alloy follows a parabolic variation in the temperature range 811 K to 922 K (538 °C to 649 °C). A drastic increase in α -case depth occurs above 811 K (538 °C) under static thermal exposure, which could be much more pronounced under dynamic conditions, setting the maximum service temperature limit of Ti-6242. The activation energy for the diffusion of oxygen in the α phase of Ti-6Al-2Sn-4Zr-2Mo is estimated as 244 kJ/mol in the temperature range 811 K to 922 K (538 °C to 649 °C).

This work was performed under United States Air Force Contract No. FA8650-10-D-5226 at the Materials and Manufacturing Directorate, United States Air Force Research Laboratory (Wright-Patterson AFB, OH). The authors acknowledge Dr. Fred Meisenkothen, UES, Inc., for his assistance with the EPMA analysis. The authors are grateful to the members of the anonymous review committee for their constructive comments, which helped the authors to include additional analyses in this article.

REFERENCES

1. H. Conrad: *Prog. Mater. Sci.*, 1981, vol. 26, pp. 138–43.
2. J.L. Murray and H.A. Wriedt: in *Binary Alloy Phase Diagrams*, T.B. Massalski, ed., ASM INTERNATIONAL, Materials Park, OH, 1990, pp. 2924–26.
3. K.S. Chan, M. Koike, B.W. Johnson, and T. Okabe: *Metall. Mater. Trans. A*, 2008, vol. 39A, pp. 171–80.
4. D. Jordan: *Heat Treating Prog.*, 2008, pp. 45–47.
5. *Metallography and Microstructures*, vol. 9, *ASM Handbook*, G.F. Vander Voort, ed., ASM INTERNATIONAL, Materials Park, OH, 2004, pp. 899–917.
6. J.C. Williams, A.W. Sommer, and P.P. Tung: *Metall. Trans.*, 1972, vol. 3, pp. 2979–84.
7. G. Lütjering and J.C. Williams: *Titanium*, 2nd ed., Springer-Verlag, Berlin, 2007, pp. 50–52.
8. R.N. Shenoy, J. Unnam, and R.K. Clark: *Oxid. Met.*, 1986, vol. 26, pp. 105–24.
9. C. Leyens and M. Peters: *Titanium and Titanium Alloys*, Wiley-VCH Verlag GmbH, Weinheim, 2003, pp. 187–230.
10. C.E. Shamblen and T.K. Redden: in *The Science, Technology, and Application of Titanium*, R.I. Jaffee and N.E. Promisel, eds., Pergamon Press, Oxford, United Kingdom, 1968, pp. 199–208.
11. I. Gurrappa: *J. Mater. Sci. Lett.*, 2003, vol. 22, pp. 771–74.
12. C. Leyens, M. Peters, D. Weinem, and W.A. Kaysser: *Metall. Mater. Trans. A*, 1996, vol. 27A, pp. 1709–17.
13. ATI Ti-6242 Technical data sheet, <http://www.alleghenytechnologies.com/allvac/pages/PDF/tech/TI-051%20Ti-6Al-2Sn-4Zr-2Mo%20.pdf>.
14. Aerospace Material Specification 4976G, SAE International, Warrendale, PA, 2008.
15. M. Uchic: United States Air Force Research Laboratory, WPAFB, OH, private communication, 2010.